Deep–Sea Research I 197 (2023) 104039

Contents lists available at ScienceDirect

Deep-Sea Research Part I

journal homepage: www.elsevier.com/locate/dsri

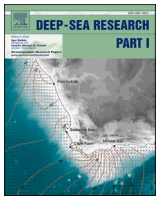

Geochemical and geochronological constraints on the tectonic and magmatic evolution of the southwestern Mariana subduction zone

Ji Zhang [a,b], Guoliang Zhang [a,b,*], Jonny Wu [c]

[a] Center of Deep Sea Research, Institute of Oceanology, Chinese Academy of Sciences, Qingdao, 266071, China
[b] Center for Ocean Mega-Science, Chinese Academy of Sciences, Qingdao, 266071, China
[c] Department of Earth and Atmospheric Sciences, University of Houston, Houston, TX, 77004, USA

ARTICLE INFO

Keywords:
Boninitic greenstones
Post-collisional magmatism
Yap–Mariana junction
Plateau–arc interaction

ABSTRACT

Interaction of a subduction zone with an oceanic plateau has implications for plate tectonics. However, the geodynamic processes and petrological responses to oceanic plateau–arc interactions remain enigmatic. The southwestern Mariana and Yap arcs have experienced interactions with the Caroline Plateau, which have affected the regional tectonism. In this study, tholeiitic basalts and metamorphosed volcanic rocks (i.e., greenstones) were recovered from the southwestern Mariana forearc. The protoliths of the metamorphosed volcanic rocks have geochemical affinities to low-silica boninites. These boninitic rocks have similar K–Ar and apatite U–Pb ages of *ca.* 24 Ma, which record the timing of collision between the southwestern Mariana arc and the Caroline Plateau. $^{40}Ar/^{39}Ar$ dating of plagioclase in the tholeiitic basalts dates post-collisional magmatism to *ca.* 18 Ma. The tholeiites have geochemical signatures of fore-arc basalts (e.g., low Ti/V ratios and light rare earth element-depleted patterns) and high Th/Yb ratios, which reflect a depleted mantle source with a subduction component inherited from a pre-collisional subduction event. We suggest that the southwestern Mariana arc is an intra-oceanic arc that underwent plateau–arc collisions. These plateau–arc interactions affected the tectonic and magmatic evolution of the southwestern Mariana arc and nearby western Pacific basins.

1. Introduction

The western Pacific comprises a number of intra-oceanic subduction zones and oceanic plateaus. At convergent margins, an oceanic plateau either subducts beneath a trench or collides with an island arc (Schellart and Rawlinson, 2010). The fate of oceanic plateaus at subduction zones is important for understanding plate tectonics throughout Earth's history (Liu et al., 2021). The Yap and Mariana trenches and Parece Vela Rift form an apparent T–T–R triple junction (Fig. 1a). The nearly E–W-trending southernmost Mariana Trench is considered to have formed in response to the collision between the Caroline Plateau and the southwestern Mariana arc (Fan et al., 2022; McCabe and Uyeda, 1983; Zhang and Zhang, 2020), which may have caused the development of the deepest trench in the Mariana arc and affected the regional tectonism. However, the timing and processes controlling this collisional event are poorly constrained.

The convergence in the Mariana region has resulted in the multi-stage formation of volcanic arcs and extensional back-arc basins, forming a series of volcanic arcs along the eastern margin of the Philippine Sea Plate. The tectonic evolution of the Izu–Bonin–Mariana (IBM) subduction zone since its initiation at *ca.* 52 Ma is complex. The early arc crust has been largely preserved along the IBM arc front (Reagan et al., 2017). Forearc basalts (FABs) and boninites are early-stage arc magmas generated shortly after subduction initiation (Arculus et al., 2015; Reagan et al., 2010). The FABs in the Mariana region formed by decompression melting of asthenospheric mantle with a negligible contribution from the subducting slabs. The appearance of boninitic magmas during subduction initiation marks the transition from decompression to fluid-assisted sub-arc mantle melting (Li et al., 2019).

Because the interactions between the southern Mariana arc and the Caroline Plateau are poorly understood, the nature of subduction initiation and evolution in the southernmost Mariana region remains unclear. The factors that controlled the evolution of the southwestern Mariana subduction zone have been little studied. The collision of the Caroline Plateau with the southernmost Mariana and Yap arcs provides an ideal opportunity to investigate the interactions between an oceanic plateau and a subduction zone. In this paper, we report geochemical and geochronological data for rock samples from the southwestern Mariana

* Corresponding author. Center of Deep Sea Research, Institute of Oceanology, Chinese Academy of Sciences, Qingdao, 266071, China.
E-mail address: zhangguoliang@qdio.ac.cn (G. Zhang).

https://doi.org/10.1016/j.dsr.2023.104039
Received 28 October 2022; Received in revised form 26 March 2023; Accepted 28 March 2023
Available online 5 April 2023

subduction zone, which are used to constrain the tectonic and magmatic history of the southernmost Mariana subduction zone.

2. Geological setting and samples

2.1. Geological setting

The southwestern Mariana subduction zone is a convergent margin between the Philippine Sea, Pacific, and Caroline plates (Fig. 1a). The Caroline Plate may have been an independent microplate that rotated counterclockwise relative to the Pacific Plate (Gaina and Müller, 2007; Hall, 2002) or that has moved with the Pacific Plate for most of its existence (Wu et al., 2016; Yan and Kroenke, 1993). The Caroline Basin, including the West Caroline and Kiilsgaard troughs, formed during the late Eocene to Oligocene (36–25 Ma) as a N–S-spreading back-arc basin (Gaina and Müller, 2007). The Caroline Plateau consists mainly of the East Caroline and West Caroline ridges, which are separated by the Sorol Trough (Fig. 1a). The Caroline Plateau was formed on the Caroline Plate from 33 to 15 Ma by a mantle plume as the Pacific Plate migrated to the northwest (Keating et al., 1984; Zhang et al., 2020a, 2020b).

The West Philippine Basin opened between 55 and 52 and 30 Ma (Deschamps and Lallemand, 2002). The Kyushu–Palau Ridge (KPR) and West Mariana Ridge (WMR) are remnant arcs that longitudinally separate the back-arc basins of the Shikoku Basin (SB), Parece Vela Basin (PVB), and Mariana Trough (Fig. 1a). The IBM convergent margin is one of the most extensively studied intra-oceanic subduction systems, and subduction along this margin began at *ca.* 52 Ma (Ishizuka et al., 2011a; Reagan et al., 2010). Boninites (48–44 Ma) are exposed sporadically along the IBM arc, which extends in a nearly N–S direction for thousands of kilometers along the eastern margin of the Philippine Sea Plate. The boninites were generated during the incipient stage of subduction in the early Paleogene. The KPR was active between 48.5 and 22.4 Ma (Ishizuka et al., 2011b). Arc volcanism on the Palau Islands was active from 40 to 20 Ma (Cosca et al., 1998; Meijer et al., 1983). Back-arc spreading that began at *ca.* 30 Ma created the Parece Vela and Shikoku back-arc basins (Ishizuka et al., 2011b), resulting in the KPR becoming a remnant arc (Okino et al., 1998). Seafloor spreading in the PVB ceased at *ca.* 15 Ma (Okino et al., 1999). The WMR was active from 20 to 9 Ma, and volcanism along the WMR is thought to have ceased at *ca.* 7 Ma (Scott et al., 1980).

2.2. Sampling

In this study, the forearc slope in the southwestern Mariana subduction zone was surveyed using the remotely operated vehicle (ROV) *Faxian* on the research vessel *KEXUE* during the 1602 cruise in 2016. Two main lithologies (volcanic and metamorphic rocks) were recovered from six diving sites at depths of 750–1800 m (Fig. 1b) that are exposed on the inner slope of the southernmost Mariana Trench. Our diving on the southern forearc terranes recovered volcanic rocks on the shallow forearc slope and metamorphic rocks on the deeper slope (Fig. 2). Phenocrysts in the volcanic rocks are mainly plagioclase, clinopyroxene, and Fe–Ti oxides, and the groundmass is mainly glassy to microcrystalline and contains plagioclase, clinopyroxene, Fe–Ti oxides, and minor quartz (Fig. 2a–c). In the metamorphic rocks, the primary mineralogy has been overprinted by an actinolite–tremolite–plagioclase–epidote–chlorite–apatite–quartz metamorphic mineral assemblage that is typical of lower to medium greenschist-facies metamorphism (Fig. 2d–f). These samples are generally green in color and have no obvious foliation and lineation, and thus are termed “greenstones” in this paper.

3. Analytical methods

Major elements were analyzed on fused glass discs using a Thermo ARL 9900 X-ray fluorescence spectrometer at the State Key Laboratory for Mineral Deposits Research, Nanjing University, Nanjing, China. Loss-on-ignition (LOI) values were determined on sample powders heated to 1000 °C. Trace elements were analyzed by inductively coupled plasma mass spectrometry (ICP–MS) at the Institute of Crustal Dynamics, China Earthquake Administration, Beijing, China. To remove the effects of seafloor weathering, the sample powders for Sr–Nd–Pb–Hf isotope analyses were leached in 6 N HCl at 70 °C for 1 h prior to digestion. After

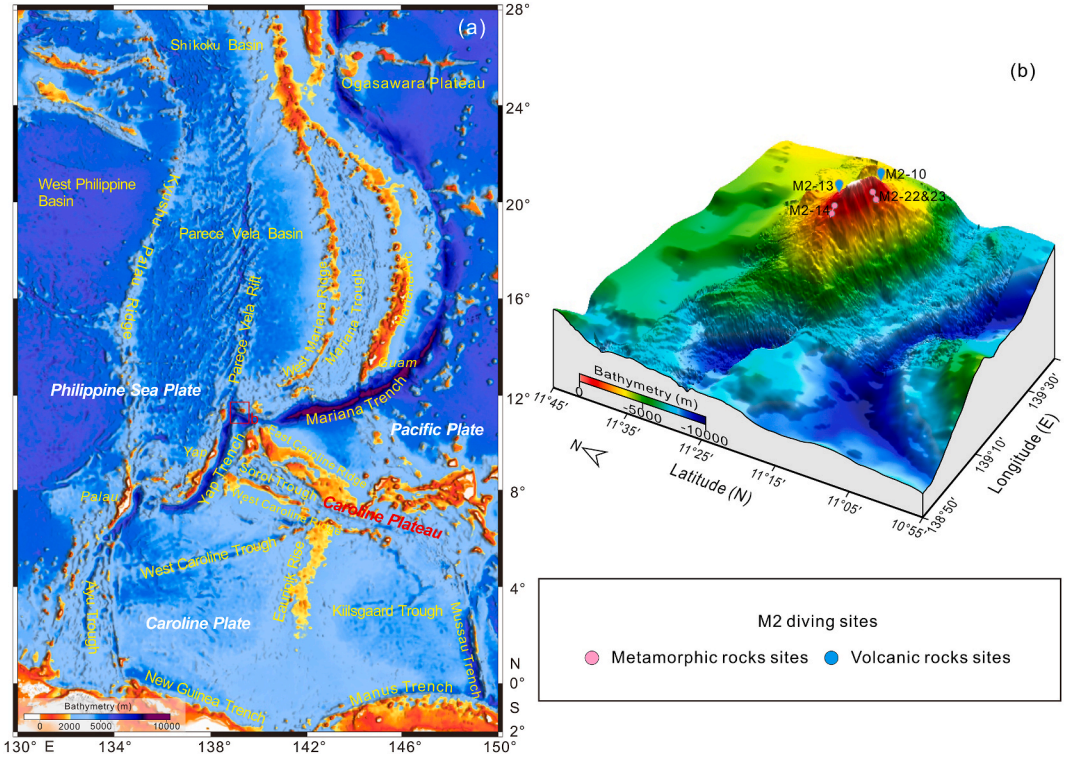

Fig. 1. (a) Bathymetric map of the boundary between the Philippine Sea, Caroline, and Pacific plates. (b) Three-dimensional view of the M2 diving sites.

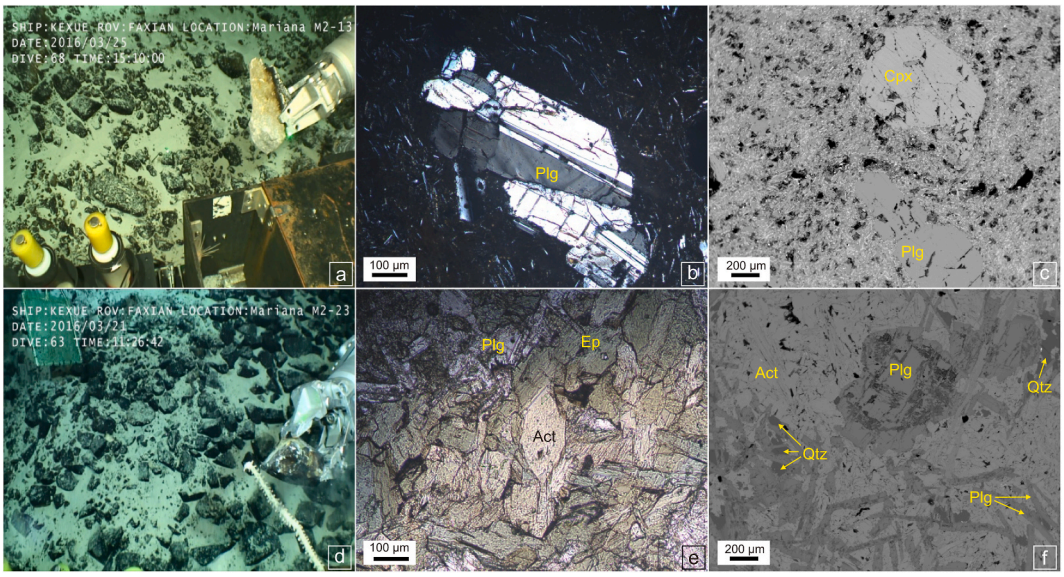

Fig. 2. Photographs of the seafloor at the (a) volcanic and (d) metamorphic rock diving sites. Photomicrographs and back-scattered electron images of representative (b–c) volcanic rock sample M2-13-3 and (e–f) metamorphic rock sample M2-22-2.

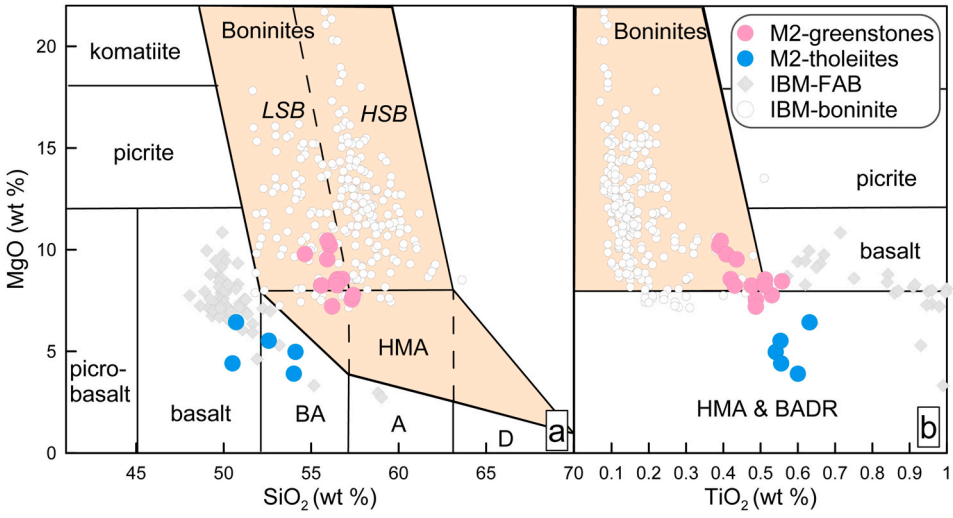

Fig. 3. Plots of (a) MgO versus SiO_2 and (b) TiO_2 versus MgO for the studied samples. Boninites were defined by Pearce and Reagan (2019) as having MgO >8 wt%, TiO_2 < 0.5 wt%, and SiO_2 > 52 wt% (the shaded fields on both diagrams). Data for the Izu–Bonin–Mariana forearc basalts (IBM FABs) are from Ishizuka et al. (2011a) and Reagan et al. (2010). Data for the Izu–Bonin–Mariana boninites (IBM boninites) are from Li et al. (2019), Shervais et al. (2021), and the Georoc database (http://georoc.mpch-mainz.gwdg.de/georoc/). The major elements were recalculated on an anhydrous basis.

chemical separation, Sr–Nd–Pb–Hf isotopes were analyzed by multi-collector ICP–MS (MC–ICP–MS) using a Nu Plasma instrument at the University of Queensland, Brisbane, Australia. Potassium–Ar dating of whole-rock samples was undertaken at the Institute of Geology, China Earthquake Administration, Beijing, China. Fresh plagioclase grains were selected for $^{40}Ar/^{39}Ar$ dating at the University of Melbourne, Melbourne, Australia, after the sample had been crushed and sieved to a grain size of 100–180 μm. Apatite U–Pb dating was undertaken at the Beijing Quick Thermo Science & Technology Company Limited, Beijing, China, using an ESI New Wave NWR 193UC laser ablation system coupled to an Agilent 8900 Triple Quadrupole ICP–MS (ICP–QQQ). Details of the analytical procedures for major and trace element analysis, isotope analysis, and dating are provided in the Supplementary Methods.

4. Results

4.1. Geochemistry

4.1.1. Metamorphic rocks

Two petrological groups of rocks (metamorphic and volcanic) were recovered from the diving sites. In the metamorphic group, the greenstones are calc-alkaline basalts and characterized by high MgO and low TiO_2 contents (Figs. S1–S2). The protoliths of these greenstone samples are low-silica boninites (LSBs) with TiO_2 = 0.36–0.56 wt% and MgO = 6.94–9.73 wt% (Fig. 3 and S2). These boninitic greenstones are characterized by high Cr contents (221–1562 ppm), high Mg# values (molar Mg/[Mg + Fe], with all Fe as Fe^{2+}; 41–55), and CaO/Al_2O_3 = 0.31–0.73 (Table S1). Primitive mantle-normalized trace element and chondrite-normalized rare earth element (REE) patterns are shown in Fig. 4a and b. The boninitic greenstones have unusually low incompatible trace element contents, with significant light REE depletions (La_N/Sm_N = 0.26–0.62) and are slightly more depleted than FABs from the IBM forearc (La_N/Sm_N = 0.27–0.83). The samples also have low Ti/V ratios (14–16; Fig. 5a), which distinguish these rocks from subducting Pacific

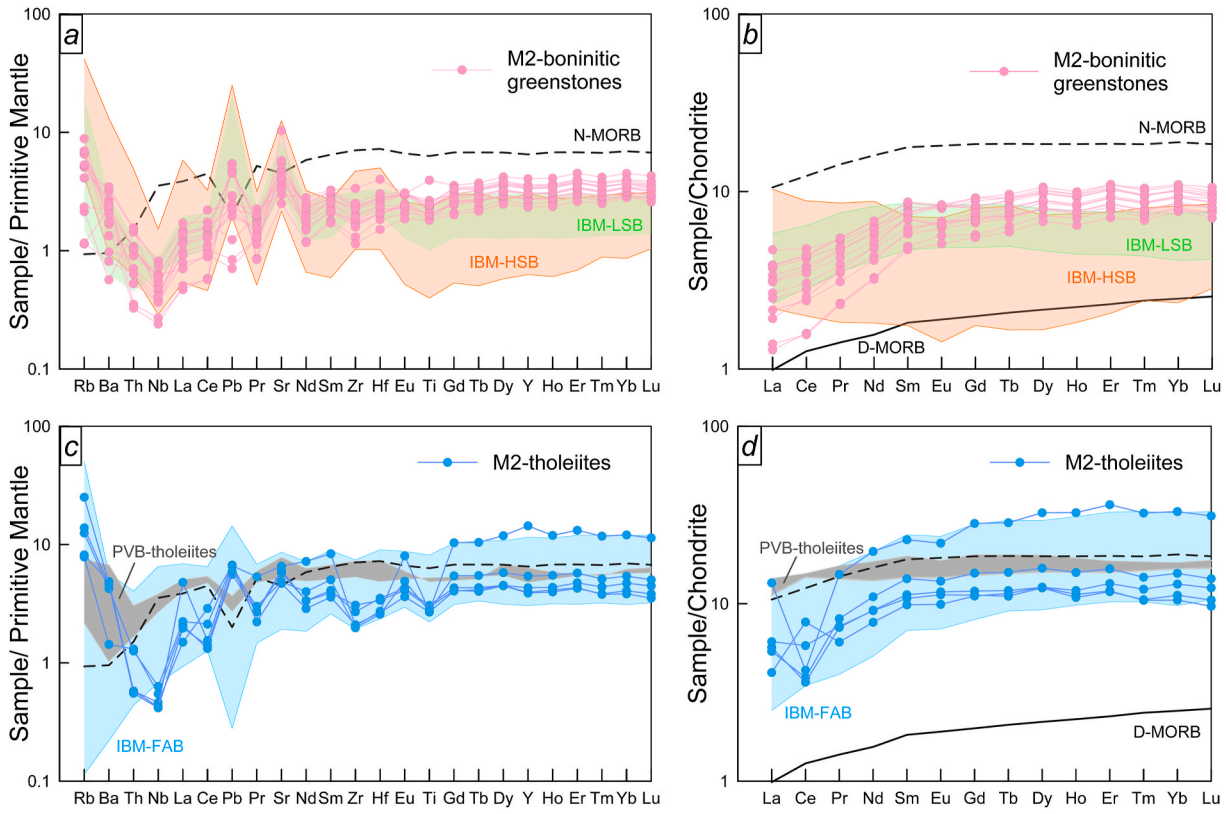

Fig. 4. Primitive mantle-normalized trace element patterns and C1 chondrite-normalized REE patterns for the (a–b) boninitic greenstone and (c–d) tholeiite samples from the M2 diving sites. Normalizing values were taken from (McDonough and Sun, 1995). The data for back-arc basin basalts in the Parece Vela Basin (DSDP Sites 449 and 450) are from Hickey-Vargas (1998). Data for typical N-MORBs and D-MORBs are from Sun and McDonough (1989) and Salters and Stracke (2004), respectively.

mid-ocean ridge basalts (MORBs; Ti/V = 26–32) and Philippine Sea MORBs (Ti/V = 17–25). Incompatible trace element ratios (e.g., Nb/Yb and Th/Yb) plot mostly in the intra-oceanic arc field (Fig. 5c). The analyzed samples have average $^{206}Pb/^{204}Pb$ = 18.61 ± 0.08, $^{208}Pb/^{204}Pb$ = 38.22 ± 0.05, and $^{207}Pb/^{204}Pb$ = 15.55 ± 0.02 (Fig. S3). These boninites have $^{87}Sr/^{86}Sr$ = 0.704179–0.707714 and $^{143}Nd/^{144}Nd$ = 0.513123–0.513181 (average = 0.513147), corresponding to εNd = 9.47–10.58 (average = 9.92). The boninites have $^{176}Hf/^{177}Hf$ = 0.283242–0.283436 (average = 0.283328), corresponding to εHf = 16.64–23.48 (average = 19.67; Fig. 6a). High εHf values are coupled with low La_N/Sm_N and Zr/Ti ratios (Fig. 6b and c), similar to the depleted mantle source of FABs in the IBM forearc.

4.1.2. Volcanic rocks

The volcanic rocks are tholeiitic basalts (FeO*/MgO = 0.9–3.0; Fig. S1), with SiO_2 = 49.5–54.1 wt%, Al_2O_3 = 17.2–18.6 wt%, CaO = 11.0–12.5 wt%, and MgO = 3.9–6.3 wt% (Fig. S2). Nickel and Cr contents range from 30.8 to 44.5 and 22.8–73.7 ppm, respectively (Table S1). All of the tholeiites have similar trace element patterns to forearc basalts (Fig. 4c). The REE patterns (Fig. 4d) are like those of normal MORBs (N-MORB), with most La/Yb ratios varying between 0.5 and 0.9. The Ti/V and Yb/V ratios of these tholeiitic basalts are distinctly lower than the PVB basalts (Fig. 5a and b). Their low Ti/V (9.1–12.6) and Yb/V (0.0051–0.0074) values are indicative of a subduction-related setting, similar to that of FABs from the southern Mariana forearc (Reagan et al., 2010). The tholeiites have higher Th/Yb ratios than MORB–OIB array and plot in the arc volcanic rock field (Fig. 5c). The analyzed samples have average $^{206}Pb/^{204}Pb$ = 18.55 ± 0.06, $^{208}Pb/^{204}Pb$ = 38.18 ± 0.04, and $^{207}Pb/^{204}Pb$ = 15.55 ± 0.01. The tholeiites have $^{87}Sr/^{86}Sr$ = 0.703394–0.704103, indicative of a minor subduction component. The volcanic rocks have $^{143}Nd/^{144}Nd$ = 0.513133–0.513168 (εNd = 9.7–10.3) and $^{176}Hf/^{177}Hf$ = 0.283326–0.283386 (εHf = 19.6–21.7; Fig. 6a). The high $^{143}Nd/^{144}Nd$ and $^{176}Hf/^{177}Hf$ ratios are indicative of a highly depleted mantle source.

4.2. Geochronology

4.2.1. Ages of the tholeiites

Fresh plagioclase grains (sample M2-13-3) were $^{40}Ar/^{40}Ar$ dated. Two plagioclase aliquots from sample M2-13-3 yielded nearly flat ^{39}Ar release spectra and plateau ages of 18.76 ± 0.79 (2σ) and 16.89 ± 0.70 Ma (2σ), respectively (Fig. 7a and b; Table S2). These ages are much younger than those of the northern IBM forearc basalts, which are considered to have formed at *ca.* 52 Ma (Reagan et al., 2019).

4.2.2. Ages of the boninitic greenstones

Sample M2-10-7 was selected for K–Ar dating (Table 1) and yielded an age of 24.50 ± 0.77 Ma. Apatite from a boninitic greenstone (sample M2-22-2) was U–Pb dated (Table S3). The U contents of the apatite vary from 1.26 to 6.23 ppm, with Th/U = 1.59–2.36. On a Tera–Wasserburg inverse U–Pb concordia diagram (Fig. 7c), the data (uncorrected for common Pb) define a linear array with a lower intercept age at 23.9 ± 3.6 Ma (2σ; MSWD = 1.9). The implications of these ages are discussed later in this paper.

5. Discussion

5.1. Effects of seafloor alteration and regional metamorphism on whole-rock geochemistry

Evaluation of the effects of alteration and metamorphism on the geochemical compositions of the studied samples is required before

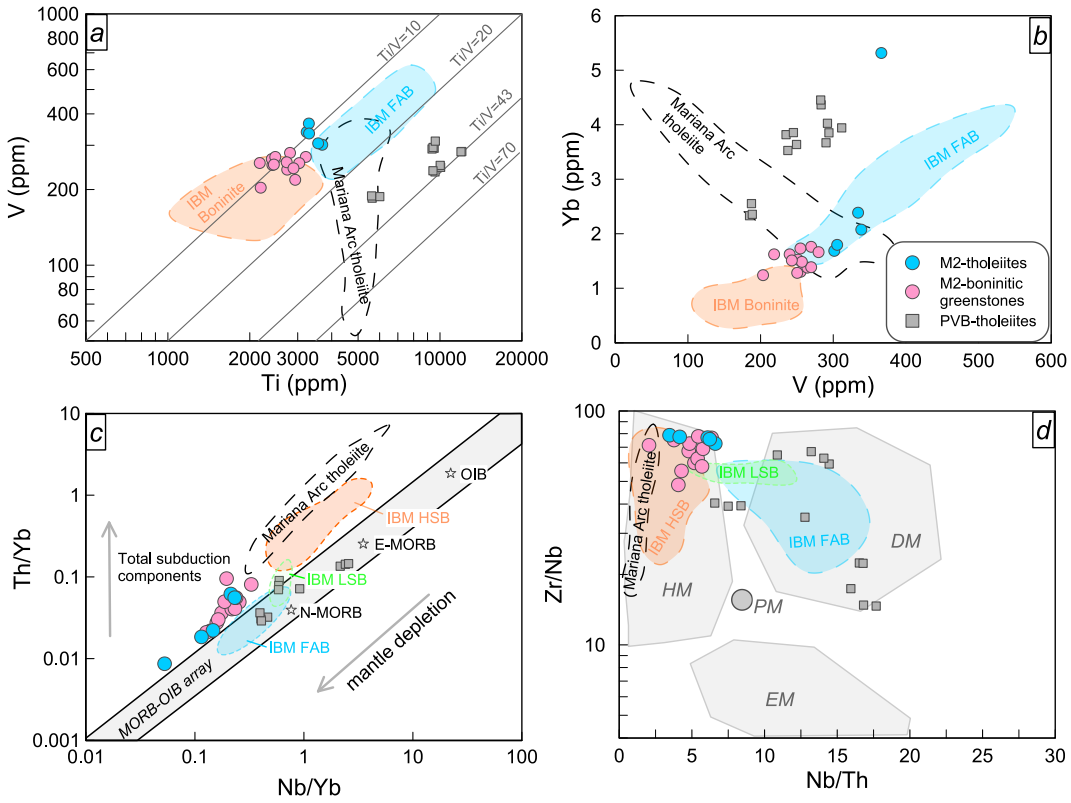

Fig. 5. Plots of (a) V versus Ti (after Shervais (2022), (b) Yb versus V, (c) Th/Yb versus Nb/Yb, and (d) Zr/Nb versus Nb/Th (after Condie (2005) for samples from the M2 diving sites. Abbreviations: PM, primitive mantle; DM, depleted mantle; HM = hydrous mantle; EM = enriched mantle. Data for the Mariana arc tholeiites were downloaded from the Georoc (http://georoc.mpch-mainz.gwdg.de/georoc/Entry.html) and PetDB (www.earthchem.org/petdb) databases. The other data sources are the same as in Figs. 3 and 4.

further discussion of the petrogenesis and source of the studied rocks. The LOI values of the studied rocks indicate the presence of volatiles and may suggest there has been some alteration. The tholeiitic samples have low LOI values (mostly <2 wt%), but some greenstone samples have relatively high LOI values (up to 6.2 wt%). The lower LOI values of the tholeiitic samples suggest these rocks were little affected by alteration. Secondary minerals were rare or not identified in thin-sections of the tholeiitic samples (Fig. 2b). In contrast, the greenstone samples have undergone low-degree greenschist face metamorphism without foliation and lineation. These greenstone samples are primarily composed of actinolite–tremolite–plagioclase–epidote–chlorite–quartz mineral assemblage. The secondary minerals affected by alteration processes were not identified in the thin sections of greenstone samples. The H_2O-bearing actinolite and epidote account more than 80% of the rock samples. Thus, the relatively high LOI values of these greenstone samples were formed during the low-degree metamorphism, rather than during the seafloor alteration.

In general, most large-ion lithophile elements (LILEs; e.g., K, Rb, Ba, and Sr) are mobile elements, whereas REEs, high-field-strength elements (HFSEs; e.g., Zr and Hf), and transition metal elements (e.g., Cr, Ni, and V) are relatively immobile (Pearce and Peate, 1995; Pearce and Reagan, 2019; Wang and Zhang, 2022) and can thus be used to evaluate the effects of regional metamorphism on whole-rock geochemistry. Zirconium was plotted against selected major elements, such as SiO_2, TiO_2, Al_2O_3, MgO, Na_2O, and Fe_2O_3 for the greenstone samples (Fig. S4). Most of these plots (especially SiO_2, TiO_2, Al_2O_3, and MgO) exhibit good linear correlations, which indicate that the greenstone samples preserve the protolith geochemistry. Plots of Nb and Zr versus other elements (Fig. S5) are used here to evaluate the trace element mobility (Jin et al., 2019; Zhang et al., 2016). The Th, La, Nd, and Yb have good correlations with Nb and Zr (Fig. S5). The good linear correlation between Zr and Ti is consistent with HFSE immobility. In addition, all the greenstone samples lack Ce anomalies (Fig. 4b), suggesting that the REE systematics were not significantly modified by low-degree metamorphism and/or seafloor alteration (Polat et al., 2003). Therefore, although the greenstone samples have experienced variable degrees of greenschist-facies metamorphism, they retain the geochemical characteristics of their protolith, especially for the REEs and HFSEs.

5.2. Origin of the boninitic greenstones

The slope top of the southwestern Mariana Trench comprises a lower metamorphic unit (boninitic greenstones) and an upper volcanic unit (tholeiites). The protoliths of the boninitic greenstones are low-silica boninites, which are depleted in HFSEs. Significant light REE depletions (La_N/Sm_N = 0.26–0.62), coupled with high εHf (16.64–23.48) and εNd (9.48–10.58) values, indicate that the low-silica boninites were derived from a strongly depleted mantle source, similar to that of FABs from the IBM forearc. The Hf and Nd isotopic compositions of convergent margin igneous rocks are considered to best preserve the composition of their mantle source (Hickey-Vargas et al., 1995) compared with other isotopic tracers (e.g., Pb and Sr), as Hf and Nd are relatively insensitive to the effects of aqueous fluids released from the subducting plate (Pearce et al., 1999; Woodhead et al., 2001). Woodhead et al. (2012) identified an ultra-depleted upper mantle component with εHf >20 and εNd >10. These isotopic compositions are rare because of their extremely refractory nature. Such source rocks have already been melted at least once, which fractionates the Lu–Hf from the Sm–Nd isotopic systems because Lu is retained in mantle garnet whereas Sm enters the melt (Salters et al., 2011). Over time, these processes result in oceanic lithosphere with highly radiogenic Hf isotopic compositions.

The appearance of boninitic magmas during subduction initiation

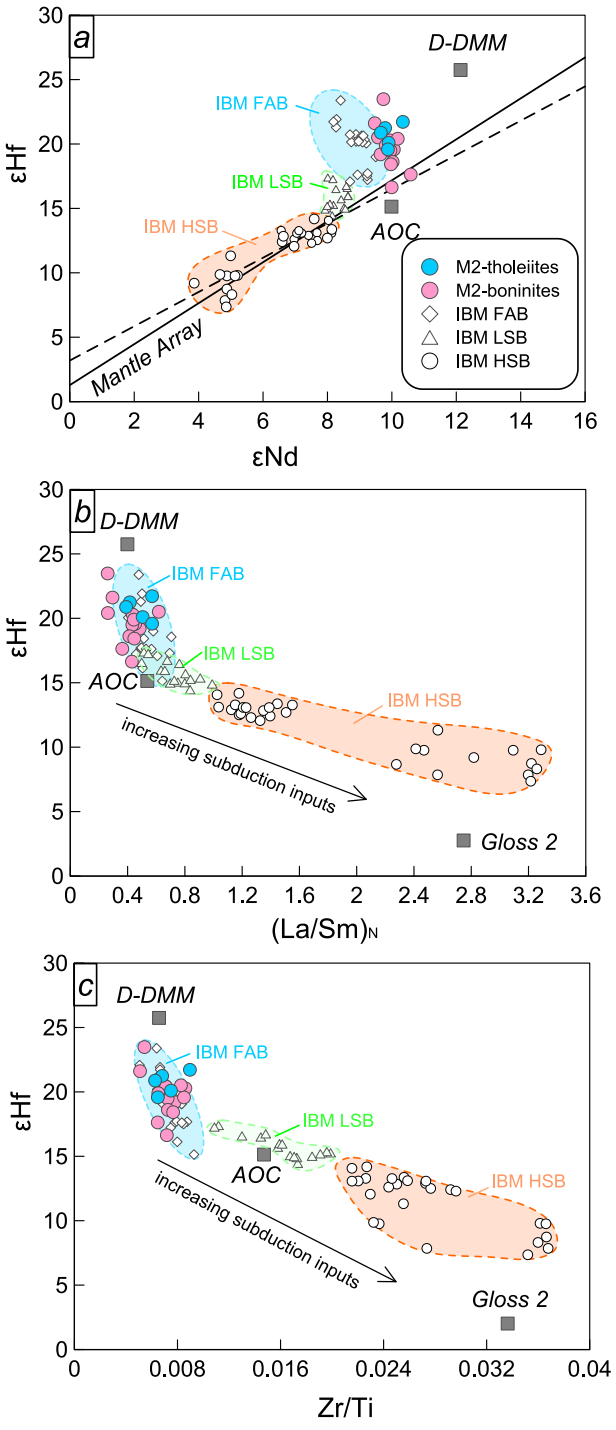

Fig. 6. Plots of (a) εHf versus εNd, (b) εHf versus $(La/Sm)_N$, and (c) εHf versus Zr/Ti for samples from the M2 diving sites. εHf is normalized to a CHUR $^{176}Hf/^{177}Hf$ value of 0.282772 (Blichert-Toft et al., 1997). Reference data: D-DMM = Salters and Stracke (2004); GLOSS = global subducting sediment of Plank and Langmuir (1998); AOC = altered oceanic crust of Chauvel et al. (2009).

marks the transition from decompression to fluid-assisted mantle melting. The relative enrichment of Pb and Sr (Fig. 4) and relatively high Sr isotope ratios (Fig. S3) can be explained by the addition of subduction components, including aqueous fluids and/or silicate melts from the subducting slab (Falloon and Danyushevsky, 2000). Low-Si boninites and High-Si boninites in the IBM subduction zones show distinctive REE pattern, including the depleted patterns and U-shaped patterns (Fig. 4b).

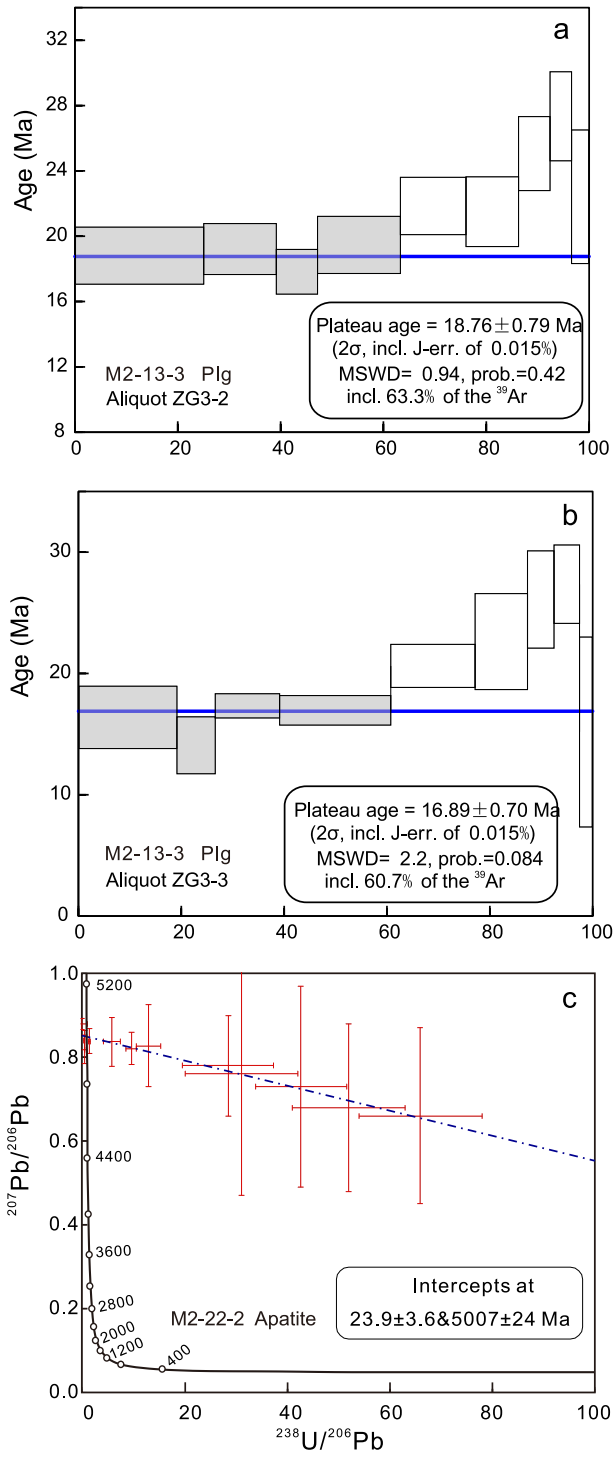

Fig. 7. (a–b) $^{40}Ar/^{39}Ar$ age spectra for plagioclase from igneous sample M2-13-3. (c) Apatite U–Pb dating results for metamorphic sample M2-22-2.

Table 1
Dating results for samples from the M2 diving sites.

Rock type	Sample	Age	Methods
Tholeiite	M2-13-3	18.76 ± 0.79 Ma (2σ) 16.89 ± 0.70 Ma (2σ)	Plg Ar–Ar
Boninitic greenstones	M2-10-7	24.50 ± 0.77 Ma	K–Ar
	M2-22-2	23.9 ± 3.6 Ma	Apatite U–Pb

The distinctive U-shaped REE patterns of HSB have been accounted for in a two stage process: depletion and refertilization (Pearce and Arculus, 2021)). In the depletion stage, high-degrees of anhydrous partial melting of upper mantle leaves a residue more depleted and refractory than the typical source of mid-ocean-ridge basalts (MORB). LSB that formed in this stage have the depleted REE patterns ($La_N/Sm_N < 1$). During the refertilization stage, the non-conservative elements Th, LREE, and MREE are transferred in hydrous fluids and/or melts from the subducting slab to the refractory residue. This two-stage process yields HSB are characterized by U-shaped REE pattern, which have higher La_N/Sm_N (Pearce and Arculus, 2021; Pearce and Robinson, 2010). Significant light REE depletions ($La_N/Sm_N = 0.26–0.62$) of the boninitic protoliths can be explained by the high degree of depletion during the subduction initiation. The high εHf values coupled with low La_N/Sm_N and Zr/Ti ratios indicate that the boninitic protoliths were derived from a strongly depleted mantle source (Fig. 6), similar to that of FABs from the IBM forearc. Low heavy REE contents and Zr/Ti ratios also provide evidence that the source was originally strongly depleted in incompatible elements. The precise concentration of any incompatible element is primarily controlled by the prior depletion in the mantle source and the subsequent addition of an enriching component. The forearc basalts, low-silica boninites and high-silica boninites (FAB–LSB–HSB) rock sequence in the Mariana subduction zone reflects an increasing contribution from the subducting slab during arc maturation (Ribeiro et al., 2020). We suggest that the protoliths of the greenstone samples are LSBs generated during subduction initiation in the proto-Mariana forearc region.

McCabe and Uyeda (1983) suggested that collision of the Ogasawara and Caroline plateaus with the Mariana Trench could explain the curvature and rotation of the Mariana arc. Our previous study showed that amphibolites in the Yap Arc formed at *ca*. 21 Ma as a result of the collision between the Caroline and Philippine Sea plates (Zhang and Zhang, 2020). Therefore, the boninitic greenstones record the complex tectonic evolution history related to collision of the Caroline Plateau with the southwestern Mariana subduction zone. In this study, new dating results for the boninitic greenstones yielded an apatite U–Pb age of 24.50 ± 0.77 Ma and a whole-rock K–Ar age of 23.9 ± 3.6 Ma. In the IBM volcanic system, the initiation of subduction was marked by the eruption of FABs during 52–48 Ma, followed by boninitic volcanism (49–45 Ma) and tholeiitic volcanism, prior to the opening of the Shikoku and Parece Vela basins (Ishizuka et al., 2011a; Reagan et al., 2010). The protoliths of the boninitic greenstone samples are LSBs, which were probably generated in a nascent forearc setting. These rocks were metamorphosed to greenstones as a result of the collision between the nascent Mariana forearc and Caroline Plateau at *ca*. 24 Ma. The metamorphic ages of the boninitic greenstones (*ca*. 24 Ma) are older than those of metamorphic rocks in the Yap Arc (*ca*. 21 Ma). The occurrence of metamorphic rocks along the Yap Arc and southwestern Mariana forearc indicates that collision of the Caroline Plateau caused regional metamorphism along the southern margin of the Philippine Sea Plate. The incoming Caroline Plateau collided with the southwestern Mariana forearc terranes, and boninitic greenstones were generated during the collision. The uplift and erosion of the forearc crust caused exhumation of the metamorphic boninites in the southwestern Mariana forearc.

5.3. Origin of the tholeiitic basalts

Based on $^{40}Ar/^{39}Ar$ dating of plagioclase (Fig. 7), the tholeiites were erupted from 18.76 ± 0.79 to 16.89 ± 0.70 Ma after the collisional stage. They represent post-collisional magmatism and were erupted above the metamorphosed boninites. Post-collisional magmatism at convergent plate boundaries has significant implications for plate tectonics, particularly the mantle evolution beneath collisional orogenic belts (Xu et al., 2020). Geological records generated before and after a collision can be used to define the timing of a collisional event (Zheng and Wu, 2018).

The IBM FABs are tholeiitic basalts with light REE-depleted pattern, similar to normal MORBs (Ishizuka et al., 2011a; Reagan et al., 2010). A definitive geochemical feature that distinguishes FABs from MORBs has been proposed by Reagan et al. (2010), focusing on the high V contents relative to Ti contents in FABs (Ti/V = 10–15). This feature has been used to fingerprint FABs in studies of arc basement rocks and ophiolites (Ishizuka et al., 2014; Stern et al., 2012). Low Ti/V ratios are usually attributed to an origin from highly depleted (Reagan et al., 2010) or oxidizing mantle conditions during melting (Shervais, 1982). The tholeiites have a similar depleted mantle source to IBM FABs (Fig. 5a and b). The studied tholeiitic basalts have FAB-like geochemical signatures, including low Ti/V ratios and light REE-depleted patterns (Figs. 4 and 5a). The tholeiitic basalts also have low Nb/Yb ratios and high Th/Yb ratios and plot away from the MORB–ocean island basalt (OIB) mantle array toward the subduction-related Mariana arc field (Fig. 5c). This indicates that the depleted mantle source of the southwestern Mariana tholeiites was modified by subduction-derived components, including slab-derived fluids and/or melts (Pearce and Peate, 1995; Pearce, 2008). In a Nb/Th–Zr/Nb tectonic discrimination diagram (Fig. 5d), the tholeiites plot in the field for arc-related basalt derived from the mantle wedge. We propose that the subduction component (e.g., with high Th/Yb ratios) was inherited from a pre-collisional subduction event. Therefore, the post-collisional tholeiites had FAB-like parental magmas, which were likely generated by partial melting of depleted mantle metasomatized by slab-derived components.

Post-collisional magmatism is related to extensional tectonism after collision (Zheng and Chen, 2017). The formation of post-collisional magmatism is relatively controversial, with an important question being what causes the refractory mantle wedge to re-melt, as thickened orogenic belts do not become sufficiently hot for melting to commence without additional heat input. Slab detachment is likely the mechanism responsible for the formation of post-collisional magmatism (Altunkaynak, 2007; Dilek and Altunkaynak, 2007). In general, convergence between a colliding plateau and arc can continue for millions of years until the loss of slab pull owing to slab detachment (Conrad and Lithgow-Bertelloni, 2002; Zheng et al., 2022). As the slab subducts, it is subjected to increasing pressures and temperatures, which lead to subduction zone metamorphism (Poli and Schmidt, 2002). Subducted oceanic lithosphere is made markedly less buoyant by the progressive metamorphism of the mafic crust into denser amphibolitic or eclogitic rocks (Brown and Johnson, 2019). Given that subduction zone metamorphism makes the subducted crust denser, this leads to higher tensile stresses that can lead to detachment of the subducted slab. However, the accreted Caroline Plateau partly resisted the ongoing subduction owing to its anomalously thick and buoyant crust, which favored shallow slab detachment. As the plateau approached the trench, increased coupling with the overriding Philippine Sea Plate caused the upper part of the partially subducted microplate to detach from the denser sinking slab. The docking of the upper crust of the plateau and tearing of the subducted slab contributed jointly to slab detachment (Duretz et al., 2012). Slab detachment can occur at sub-arc depths, which allows hot asthenospheric material to quickly ascend into the mantle wedge that provides heat for re-melting of the shallow mantle wedge and generation of post-collisional magmatism (van de Zedde and Wortel, 2001). The ascent of asthenospheric material produces the thermal anomaly that leads to post-collisional magmatism and this stage is thought to be transient (Ferrari, 2004, 2004v; van de Zedde and Wortel, 2001), which accounts for the small amounts of such volcanic rocks in the southwestern Mariana arc. It is plausible that post-collisional volcanism occurred as a consequence of slab detachment, but further detailed geodynamic studies need to be conducted to clarify the arc–plateau interactions along the Mariana–Yap junction.

5.4. Implications for the regional tectonic evolution

Previous studies have proposed that the Caroline Plate collided with

the Philippine Sea Plate during the early Miocene (McCabe and Uyeda, 1983; Ohara et al., 2002), but considerable uncertainty remains about the mechanisms of collision between the Caroline Plateau and the southwestern Mariana subduction zone. In this study, we identified two different petrological groups, metamorphosed boninitic greenstones (*ca.* 24 Ma) and tholeiites (*ca.* 18 Ma), in the southwestern Mariana arc. The presence of boninitic greenstones shows that the southwestern Mariana arc experienced a plateau–arc collision, whereas the FAB-like tholeiites represent post-collisional volcanism. These boninitic greenstones record the collision between the southwestern Mariana forearc and the Caroline Plateau at *ca.* 24 Ma (Fig. 8a and b). There are several major regional tectonic changes that occurred at *ca.* 25 Ma that may have been related to this collisional event. At the western boundary of the Caroline Plate, the Ayu Trough opened in an E–W direction from 30 to 25 Ma, and the spreading direction changed to NW–SE during 25–16 Ma, based on sediment deposition rates and thicknesses inferred from seismic profiles (Fujiwara et al., 1995; Zhang et al., 2022). Within the Caroline Plate, important tectonic events occurred in response to the collisional event at *ca.* 25 Ma. The magnetic lineations on the Caroline Plate range in age from 35 to 25 Ma in the East Caroline Trough (Kiilsgaard Trough) and from 36 to 25 Ma in the West Caroline Trough (Gaina and Müller, 2007). The change in the spreading direction of the Ayu Trough and the spreading termination of the Caroline Basin at *ca.* 25 Ma can be attributed to the collisional event that occurred along the western boundary of the Caroline Plate. This indicates that the Caroline Plate began to transition from an extensional setting to a compressional setting at *ca.* 25 Ma. Therefore, the collisional events between the Caroline Plateau and southwestern Mariana and Yap arc systems were likely not a localized event, but part of a larger regional plate reorganization during the latest Oligocene.

In a broader tectonic context, the 24 Ma collision between the southwestern Mariana arc and the Caroline Plateau could have been related to the clockwise rotation of the Philippine Sea Plate (Deschamps and Lallemand, 2002; Weissel and Anderson, 1978). It has been debated whether the entire Philippine Sea Plate rotated substantially (~80° clockwise) or whether the rotation was due to local block deformations that only occurred along the plate margins (Wu et al., 2016). A recent paleomagnetic study of oriented cores from the plate center now confirms that the Philippine Sea Plate rotated 50° clockwise from the late Oligocene to the present (Yamazaki et al., 2021). This period of clockwise rotation immediately followed the 24 Ma collision between the southwestern Mariana forearc and the Caroline Plate and is consistent

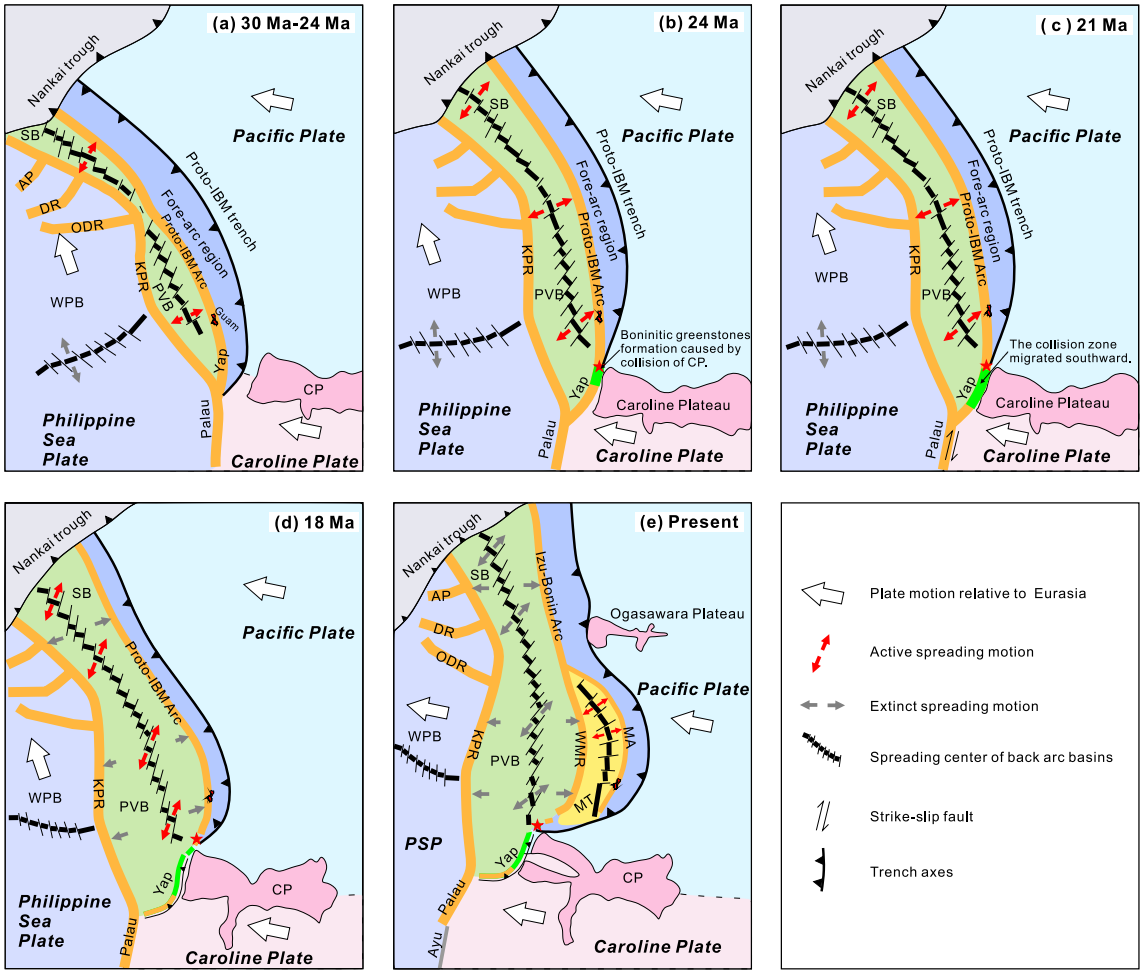

Fig. 8. Model for the tectonic evolution of the southwestern Mariana subduction zone during the (a) pre-collisional tectonic stage, (b–c) collisional tectonic stage, and (d–e) post-collisional tectonic stage. (a) Early subduction of the initial IBM Arc. Low-silica boninites (LSBs) formed during the early stage of subduction in the forearc region. (b) Collision of the proto-IBM forearc region with the incoming Caroline Plateau at *ca.* 24 Ma. LSBs of the proto-Mariana forearc crust were metamorphosed to boninitic greenstones due to the collision. (c) As the Philippine Sea Plate moved northward, the collision zone between the Caroline Plateau and forearc region migrated southward. The collision between the Caroline Plateau and proto-Yap forearc occurred at 21 Ma based on basement rocks in the Yap arc. (d) Post-collisional volcanism occurred and tholeiites formed at *ca.* 18 Ma. (e) The present-day geometry of the southwestern Mariana subduction zone. The plate motion is shown relative to stable Eurasia based on the MORVEL model (DeMets et al., 2010). AP = Amami Plateau; DR = Daito Ridge; ODR = Oki–Daito Ridge; WPB = West Philippine Basin; KPR = Kyushu–Palau Ridge; PVB = Parece Vela Basin; WMR = West Mariana Ridge.

with plate reconstructions that suggest the Caroline–Philippine Sea plate collision was a major driver of the Philippine Sea Plate rotation (Fig. 8a and b). In these models, the collision point of the Caroline Plateau migrates southward at ~12 mm/yr, based on the Pacific and Philippine Sea plate relative motion (Wu et al., 2016). In Fig. 8c, northward subduction of the Philippine Sea Plate would have allowed this collision zone to have transferred from the southwestern Mariana forearc (at *ca.* 24 Ma) to the Yap forearc (at *ca.* 21 Ma), which is consistent with the ages of metamorphic rock in the Yap forearc (Zhang and Zhang, 2020).

In the back-arc region, enigmatic changes in the spreading rate and direction of the Parece Vela and Shikoku basins could have been the result of collision–rotation between the Caroline and Philippine Sea plates. As shown by Lallemand (2016), the evolution of the PVB occurred in four stages: rifting, E–E spreading, NE–SW spreading with counterclockwise rotation of the spreading axes, and post-spreading deformation and volcanism. The abrupt change in the PVB spreading rate and direction (E–W to NE–SW spreading) occurred at 24–21 Ma (Sdrolias et al., 2004). Bathymetric and geomagnetic research (Okino et al., 1998; Sdrolias et al., 2004) has revealed that the PVB experienced E–W spreading during the Oligocene, which produced N–S-trending abyssal hills and E–W-trending transform faults along the Parece Vela Rift after *ca.* 25 Ma. During the collisional stage, the PVB experienced NE–SW spreading in the early Miocene, which produced NW–SE--trending abyssal hills and NE–SW-trending transform faults. Similar changes in spreading were observed slightly later (i.e., 19 Ma) in the Shikoku Basin (Fig. 8d), which is located >1500 km north of the southwestern Mariana subduction zone (Sdrolias et al., 2004), and this might indicate the widespread effects of the collision.

6. Conclusions

In this study, we conducted a systematic geochronological and geochemical investigation of boninitic greenstones and tholeiites from the southwestern Mariana subduction zone in order to constrain the origin and tectonic setting of the southwestern Mariana forearc and the tectonic history of the divergent margin between the Philippine Sea and Caroline plates.

The protoliths of the boninitic greenstones are depleted LSBs generated during the initiation of subduction in the proto-Mariana forearc. The presence of boninitic greenstones in the southwestern Mariana forearc demonstrates that boninitic forearc rocks were metamorphosed to greenstones at *ca.* 24 Ma, thus recording the collision between the southwestern Mariana forearc and the Caroline Plateau. After the collisional event, post-collisional magmatism occurred in the southwestern Mariana arc between 18.8 and 16.9 Ma. The resultant tholeiitic basalts are characterized by FAB-like geochemical signatures and were derived from a highly depleted mantle source. The FAB-like tholeiitic basalts that formed during the post-collisional stage lead us to propose that the collisional event caused slab break-off, which allowed hot asthenospheric mantle to ascend and melt. The studied metamorphic and volcanic rocks in the southwestern Mariana forearc record interactions between the Caroline Plateau and the southwestern Mariana arc. The collisional event caused a regional plate reorganization during the latest Oligocene, which controlled the tectonic and magmatic evolution of the southwestern Mariana arc and nearby western Pacific basins.

Declaration of competing interest

The authors declare that they have no known competing financial interests or personal relationships that could have appeared to influence the work reported in this paper.

Data availability

Data will be made available on request.

Acknowledgements

We greatly appreciate the detailed comments of two anonymous referees and Guest Editor Weidong Sun. We thank Kuidong Xu and Qing Luo of IOCAS, and the crew of the *Faxian* ROV during the R/V *KEXUE* cruise for sampling the rocks from the M2 diving sites. We thank Song Lu and David Phillips at the University of Melbourne for the $^{40}Ar/^{39}Ar$ dating. We thank Ying Wu of the Institute of Geology, China Earthquake Administration, for the K–Ar dating. We thank Jianxin Zhao at the University of Queensland for the Sr–Nd–Pb–Hf isotope analyses. This research was supported by the Strategic Priority Research Program of the Chinese Academy of Sciences (Grant XDA22050101), National Key R&D Program of China (Grant 2022YFF0801000), Marine S&T Fund of Shandong Province for Pilot National Laboratory for Marine Science and Technology (QNLM) (Grant 2022QNLM050201-3), National Natural Science Foundation of China (Grant 91858206), and China Postdoctoral Science Foundation (Grant 2022M713184). Jonny Wu was supported by the United States National Science Foundation (Grant EAR-1848327).

Appendix A. Supplementary data

Supplementary data to this article can be found online at https://doi.org/10.1016/j.dsr.2023.104039.

References

Altunkaynak, S., 2007. Collision-driven slab breakoff magmatism in northwestern Anatolia, Turkey. J. Geol. 115 (1), 63–82.
Arculus, R.J., Ishizuka, O., Bogus, K.A., Gurnis, M., Hickey-Vargas, R., Aljahdali, M.H., Bandini-Maeder, A.N., Barth, A.P., Brandl, P.A., Drab, L., Guerra, R.D., Hamada, M., Jiang, F.Q., Kanayama, K., Kender, S., Kusano, Y., Li, H., Loudin, L.C., Maffione, M., Marsaglia, K.M., McCarthy, A., Meffre, S., Morris, A., Neuhaus, M., Savov, I.P., Sena, C., Tepley, F.J., van der Land, C., Yogodzinski, G.M., Zhang, Z.H., 2015. A record of spontaneous subduction initiation in the Izu-Bonin-Mariana arc. Nat. Geosci. 8 (9), 728–733.
Blichert-Toft, J., Chauvel, C., Albarède, F., 1997. Separation of Hf and Lu for high-precision isotope analysis of rock samples by magnetic sector-multiple collector ICP-MS. Contrib. Mineral. Petrol. 127 (3), 248–260.
Brown, M., Johnson, T., 2019. Metamorphism and the evolution of subduction on Earth. Am. Mineral. 104 (8), 1065–1082.
Chauvel, C., Marini, J.-C., Plank, T., Ludden, J.N., 2009. Hf-Nd input flux in the Izu-Mariana subduction zone and recycling of subducted material in the mantle. G-cubed 10 (1), Q01001.
Condie, K.C., 2005. High field strength element ratios in Archean basalts: a window to evolving sources of mantle plumes? Lithos 79 (3), 491–504.
Conrad, C.P., Lithgow-Bertelloni, C., 2002. How mantle slabs drive plate tectonics. Science 298 (5591), 207–209.
Cosca, M.A., Arculus, R.J., Pearce, J.A., Mitchell, J.G., 1998. 40Ar/39Ar and K–Ar geochronological age constraints for the inception and early evolution of the Izu–Bonin – Mariana arc system. Isl. Arc 7 (3), 579–595.
DeMets, C., Gordon, R.G., Argus, D.F., 2010. Geologically current plate motions. Geophys. J. Int. 181 (1), 1–80.
Deschamps, A., Lallemand, S., 2002. The West Philippine Basin: an Eocene to early Oligocene back arc basin opened between two opposed subduction zones. J. Geophys. Res. Solid Earth 107 (B12).
Dilek, Y., Altunkaynak, S., 2007. Cenozoic crustal evolution and mantle dynamics of post-collisional magmatism in western Anatolia. Int. Geol. Rev. 49 (5), 431–453.
Duretz, T., Schmalholz, S.M., Gerya, T.V., 2012. Dynamics of slab detachment. G-cubed 13 (3), 1–17.
Falloon, T.J., Danyushevsky, L.V., 2000. Melting of refractory mantle at 1 center dot 5, 2 and 2 center dot 5 GPa under, anhydrous and H2O-undersaturated conditions: implications for the petrogenesis of high-Ca boninites and the influence of subduction components on mantle melting. J. Petrol. 41 (2), 257–283.
Fan, J., Zheng, H., Zhao, D., Dong, D., Bai, Y., Li, C., Zhang, Z., 2022. Seismic structure of the Caroline Plateau-Yap trench collision zone. Geophys. Res. Lett. 49 (6), 1–10.
Ferrari, L., 2004. Slab detachment control on mafic volcanic pulse and mantle heterogeneity in central Mexico. Geology 32 (1), 77–80.
Fujiwara, T., Tamaki, K., Fujimoto, H., Ishii, T., Seama, N., Toh, H., Koizumi, K., Igarashi, C., Segawa, J., Kobayashi, K., Kido, M., Seno, T., Kinoshita, H., 1995. Morphological studies of the Ayu Trough, Philippine Sea-Caroline Plate boundary. Geophys. Res. Lett. 22 (2), 109–112.
Gaina, C., Müller, D., 2007. Cenozoic tectonic and depth/age evolution of the Indonesian gateway and associated back-arc basins. Earth Sci. Rev. 83 (3–4), 177–203.
Hall, R., 2002. Cenozoic geological and plate tectonic evolution of SE Asia and the SW Pacific: computer-based reconstructions, model and animations. J. Asian Earth Sci. 20 (4), 353–431.

Hickey-Vargas, R., 1998. Origin of the Indian Ocean-type isotopic signature in basalts from Philippine Sea plate spreading centers: an assessment of local versus large-scale processes. J. Geophys. Res. Solid Earth 103 (B9), 20963–20979.
Hickey-Vargas, R., Hergt, J.M., Spadea, P., 1995. The Indian Ocean-type Isotopic Signature in Western Pacific Marginal Basins: Origin and Significance. Active Margins and Marginal Basins of the Western Pacific, pp. 175–197. American Geophysical Union.
Ishizuka, O., Tani, K., Reagan, M.K., 2014. Izu-bonin-mariana forearc crust as a modern ophiolite analogue. Elements 10 (2), 115–120.
Ishizuka, O., Tani, K., Reagan, M.K., Kanayama, K., Umino, S., Harigane, Y., Sakamoto, I., Miyajima, Y., Yuasa, M., Dunkley, D.J., 2011a. The timescales of subduction initiation and subsequent evolution of an oceanic island arc. Earth Planet Sci. Lett. 306 (3), 229–240.
Ishizuka, O., Taylor, R.N., Yuasa, M., Ohara, Y., 2011b. Making and breaking an island arc: a new perspective from the Oligocene Kyushu-Palau arc, Philippine Sea. G-cubed 12, 1–40.
Jacobsen, S.B., Wasserburg, G.J., 1980. Sm-Nd isotopic evolution of chondrites. Earth Planet Sci. Lett. 50 (1), 139–155.
Jin, X., Zhang, Y.-X., Zhou, X.-Y., Zhang, K.-J., Li, Z.-W., Khalid, S.B., Hu, J.-C., Lu, L., Sun, W.-D., 2019. Protoliths and tectonic implications of the newly discovered Triassic Baqing eclogites, central Tibet: evidence from geochemistry, SrNd isotopes and geochronology. Gondwana Res. 69, 144–162.
Keating, B.H., Mattey, D.P., Helsley, C.E., Naughton, J.J., Epp, D., Lazarewicz, A., Schwank, D., 1984. Evidence for a hot spot origin of the Caroline Islands. J. Geophys. Res. Solid Earth 89 (B12), 9937–9948.
Kempton, P.D., Pearce, J.A., Barry, T.L., Fitton, J.G., Langmuir, C., Christie, D.M., 2002. Sr-Nd-Pb-Hf isotope results from ODP leg 187: evidence for mantle dynamics of the Australian-antarctic discordance and origin of the Indian MORB source. G-cubed 3 (12), 1–35.
Lallemand, S., 2016. Philippine Sea Plate inception, evolution, and consumption with special emphasis on the early stages of Izu-Bonin-Mariana subduction. Prog. Earth Planet. Sci. 3 (1), 1–15.
Li, H.-Y., Taylor, R.N., Prytulak, J., Kirchenbaur, M., Shervais, J.W., Ryan, J.G., Godard, M., Reagan, M.K., Pearce, J.A., 2019. Radiogenic isotopes document the start of subduction in the Western Pacific. Earth Planet Sci. Lett. 518, 197–210.
Liu, Z., Dai, L., Li, S., Wang, L., Xing, H., Liu, Y., Ma, F., Dong, H., Li, F., 2021. When plateau meets subduction zone: a review of numerical models. Earth Sci. Rev. 215, 1–17.
McCabe, R., Uyeda, S., 1983. Hypothetical model for the bending of the Mariana arc. The Tectonic and Geologic Evolution of Southeast Asian Seas and Islands: Part 2, 281–293.
McDonough, W.F., Sun, S.s., 1995. The composition of the Earth. Chem. Geol. 120 (3), 223–253.
Meijer, A., Reagan, M., Ellis, H., Shafiqullah, M., Sutter, J., Damon, J., Kling, S., 1983. Chronology of volcanic events in the eastern Philippine Sea. American Geophysical Union. In: Hayes, D.E. (Ed.), The Tectonic and Geological Evolution of Southeast Asian Seas and Islands, Part 2. AGU Geophys Monogr, Washington, DC.
Ohara, Y., Fujioka, K., Ishizuka, O., Ishii, T., 2002. Peridotites and volcanics from the Yap arc system: implications for tectonics of the southern Philippine Sea Plate. Chem. Geol. 189 (1–2), 35–53.
Okino, K., Kasuga, S., Ohara, Y., 1998. A new scenario of the Parece Vela basin genesis. Mar. Geophys. Res. 20, 21–40.
Okino, K., Ohara, Y., Kasuga, S., Kato, Y., 1999. The Philippine Sea: new survey results reveal the structure and history of the marginal basins. Geophys. Res. Lett. 26, 2287–2290.
Pearce, J., Kempton, P., Nowell, G., Noble, S., 1999. Hf-Nd element and isotope perspective on the nature and provenance of mantle and subduction components in Western Pacific arc-basin systems. J. Petrol. 40 (11), 1579–1611.
Pearce, J., Peate, D., 1995. Tectonic implications of the composition of volcanic arc magmas. Annu. Rev. Earth Planet Sci. 23, 251–286.
Pearce, J.A., 2008. Geochemical fingerprinting of oceanic basalts with applications to ophiolite classification and the search for Archean oceanic crust. Lithos 100 (1), 14–48.
Pearce, J.A., Arculus, R.J., 2021. Boninites. Encyclopedia of Geology, pp. 113–129.
Pearce, J.A., Reagan, M.K., 2019. Identification, classification, and interpretation of boninites from Anthropocene to Eoarchean using Si-Mg-Ti systematics. Geosphere 15, 1–30.
Pearce, J.A., Robinson, P.T., 2010. The Troodos ophiolitic complex probably formed in a subduction initiation, slab edge setting. Gondwana Res. 18 (1), 60–81.
Plank, T., Langmuir, C.H., 1998. The chemical composition of subducting sediment and its consequences for the crust and mantle. Chem. Geol. 145 (3), 325–394.
Polat, A., Hofmann, A.W., Münker, C., Regelous, M., Appel, P.W.U., 2003. Contrasting geochemical patterns in the 3.7–3.8 Ga pillow basalt cores and rims, Isua greenstone belt, Southwest Greenland: implications for postmagmatic alteration processes. Geochem. Cosmochim. Acta 67 (3), 441–457.
Poli, S., Schmidt, M.W., 2002. Petrology of subducted slabs. Annu. Rev. Earth Planet Sci. 30 (1), 207–235.
Reagan, M., Heywood, L., Goff, K., Michibayashi, K., Foster, C., Jicha, B., Lapen, T., C McClelland, W., Ohara, Y., Righter, M., Scott, S., Sims, K., 2017. In: Geodynamic Implications of Crustal Lithologies from the Southeast Mariana Forearc.
Reagan, M.K., Heaton, D.E., Schmitz, M.D., Pearce, J.A., Shervais, J.W., Koppers, A.A.P., 2019. Forearc ages reveal extensive short-lived and rapid seafloor spreading following subduction initiation. Earth Planet Sci. Lett. 506, 520–529.
Reagan, M.K., Ishizuka, O., Stern, R.J., Kelley, K.A., Ohara, Y., Blichert-Toft, J., Bloomer, S.H., Cash, J., Fryer, P., Hanan, B.B., Hickey-Vargas, R., Ishii, T., Kimura, J.-I., Peate, D.W., Rowe, M.C., Woods, M., 2010. Fore-arc basalts and subduction initiation in the Izu-Bonin-Mariana system. G-cubed 11 (3), 1–17.
Ribeiro, J.M., Ishizuka, O., Lee, C.-T.A., Girard, G., 2020. Evolution and maturation of the nascent Mariana arc. Earth Planet Sci. Lett. 530, 1–11.
Salters, V.J.M., Mallick, S., Hart, S.R., Langmuir, C.E., Stracke, A., 2011. Domains of depleted mantle: new evidence from hafnium and neodymium isotopes. G-cubed 12 (8), Q08001.
Salters, V.J.M., Stracke, A., 2004. Composition of the depleted mantle. G-cubed 5 (5). Q05B07.
Schellart, W.P., Rawlinson, N., 2010. Convergent plate margin dynamics: new perspectives from structural geology, geophysics and geodynamic modelling. Tectonophysics 483 (1–2), 4–19.
Scott, R., Kroenke, L., Zakariadze, G., Sharaskin, A., 1980. Evolution of the South Philippine Sea: deep sea drilling project Leg 59 results. Initial Rep. Deep Sea Drill. Proj. 59, 803–815.
Sdrolias, M., Roest, W.R., Müller, R.D., 2004. An expression of philippine Sea plate rotation: the Parece Vela and Shikoku basins. Tectonophysics 394 (1–2), 69–86.
Shervais, J.W., 1982. Ti-V plots and the petrogenesis of modern and ophiolitic lavas. Earth Planet Sci. Lett. 59 (1), 101–118.
Shervais, J.W., 2022. The petrogenesis of modern and ophiolitic lavas reconsidered: Ti-V and Nb-Th. Geosci. Front. 13 (2), 101319.
Shervais, J.W., Reagan, M.K., Godard, M., Prytulak, J., Ryan, J.G., Pearce, J.A., Almeev, R.R., Li, H., Haugen, E., Chapman, T., Kurz, W., Nelson, W.R., Heaton, D.E., Kirchenbaur, M., Shimizu, K., Sakuyama, T., Vetter, S.K., Li, Y., Whattam, S., 2021. Magmatic response to subduction initiation, Part II: boninites and related rocks of the Izu-Bonin arc from IODP expedition 352. G-cubed 22 (1).
Stern, R.J., Reagan, M., Ishizuka, O., Ohara, Y., Whattam, S., 2012. To Understand Subduction Initiation, Study Forearc Crust: to Understand Forearc Crust, Study Ophiolites (Lithosphere).
Sun, S.S., McDonough, W., 1989. Chemical and isotopic systematics of oceanic basalts: implications for mantle composition and processes. Geological Society, London, Special Publications 42 (1), 313–345.
van de Zedde, D.M.A., Wortel, M.J.R., 2001. Shallow slab detachment as a transient source of heat at midlithospheric depths. Tectonics 20 (6), 868–882.
Wang, S., Zhang, G., 2022. Geochemical constraints on mantle source nature and recycling of subducted sediments in the Sulu Sea. Geosystems and Geoenvironment 1 (1), 100005.
Weissel, J.K., Anderson, R.N., 1978. Is there a Caroline plate? Earth Planet Sci. Lett. 41 (2), 143–158.
Woodhead, J., Stern, R.J., Pearce, J., Hergt, J., Vervoort, J., 2012. Hf-Nd isotope variation in Mariana Trough basalts: the importance of “ambient mantle” in the interpretation of subduction zone magmas. Geology 40 (6), 539–542.
Woodhead, J.D., Hergt, J.M., Davidson, J.P., Eggins, S.M., 2001. Hafnium isotope evidence for ‘conservative’ element mobility during subduction zone processes. Earth Planet Sci. Lett. 192 (3), 331–346.
Wu, J., Suppe, J., Lu, R., Kanda, R., 2016. Philippine Sea and East Asian plate tectonics since 52 Ma constrained by new subducted slab reconstruction methods. J. Geophys. Res. Solid Earth 121 (6), 4670–4741.
Xu, W., Zhao, Z., Dai, L., 2020. Post-collisional mafic magmatism: record of lithospheric mantle evolution in continental orogenic belt. Sci. China Earth Sci. 63 (12), 2029–2041.
Yamazaki, T., Chiyonobu, S., Ishizuka, O., Tajima, F., Uto, N., Takagawa, S., 2021. Rotation of the Philippine Sea plate inferred from paleomagnetism of oriented cores taken with an ROV-based coring apparatus. Earth Planets Space 73 (1).
Yan, C.Y., Kroenke, L.W., 1993. A plate tectonic reconstruction of the Southwest Pacific, 0–100 Ma. Proc. Ocean Drill. Progr. Sci. Results 130, 697–709.
Zhang, G.-L., Wang, S., Zhang, J., Zhan, M.-J., Zhao, Z.-H., 2020a. Evidence for the essential role of CO2 in the volcanism of the waning Caroline mantle plume. Geochem. Cosmochim. Acta 290, 391–407.
Zhang, G.-L., Zhang, J., Wang, S., Zhao, J.-X., 2020b. Geochemical and chronological constraints on the mantle plume origin of the Caroline Plateau. Chem. Geol. 540, 1–15.
Zhang, J., Zhang, G.-L., 2020. Geochemical and chronological evidence for collision of proto-Yap arc/Caroline plateau and rejuvenated plate subduction at Yap trench. Lithos 370–371, 105616.
Zhang, L., Chen, R.-X., Zheng, Y.-F., Hu, Z., Yang, Y., Xu, L., 2016. Geochemical constraints on the protoliths of eclogites and blueschists from North Qilian, northern Tibet. Chem. Geol. 421, 26–43.
Zhang, Z., Li, S., Wang, G., Suo, Y., Wang, G., Wang, P., 2022. Plate boundary processes of the Caroline Plate. Sci. China Earth Sci. 65 (8), 1554–1567.
Zheng, Y.-F., Chen, R.-X., 2017. Regional metamorphism at extreme conditions: implications for orogeny at convergent plate margins. J. Asian Earth Sci. 145, 46–73.
Zheng, Y., Chen, Y., Chen, R., Dai, L., 2022. Tectonic evolution of convergent plate margins and its geological effects. Sci. China Earth Sci. 65 (7), 1247–1276.
Zheng, Y., Wu, F., 2018. The timing of continental collision between India and Asia. Sci. Bull. 63 (24), 1649–1654.